VIP Non-Heme Iron Complexes Very Important Paper

International Edition: DOI: 10.1002/anie.201804836
German Edition: DOI: 10.1002/ange.201804836

Crystallographic Evidence for a Sterically Induced Ferryl Tilt in a Non-Heme Oxoiron(IV) Complex that Makes it a Better Oxidant

Waqas Rasheed, Apparao Draksharapu, Saikat Banerjee, Victor G. Young, Jr., Ruixi Fan, Yisong Guo, M. Ozerov, Joscha Nehrkorn, J. Krzystek, Joshua Telser,* and Lawrence Que, Jr.**

Dedicated to Professor Daryle H. Busch on the occasion of his 90th birthday

Abstract: *Oxoiron(IV) units are often implicated as intermediates in the catalytic cycles of non-heme iron oxygenases and oxidases. The most reactive synthetic analogues of these intermediates are supported by tetradentate tripodal ligands with N-methylbenzimidazole or quinoline donors, but their instability precludes structural characterization. Herein we report crystal structures of two $[Fe^{IV}(O)(L)]^{2+}$ complexes supported by pentadentate ligands incorporating these heterocycles, which show longer average Fe–N distances than the complex with only pyridine donors. These longer distances correlate linearly with $\log k_2'$ values for O- and H-atom transfer rates, suggesting that weakening the ligand field increases the electrophilicity of the Fe=O center. The sterically bulkier quinoline donors are also found to tilt the Fe=O unit away from a linear N-Fe=O arrangement by 10°.*

Bioinorganic chemists have mounted a significant effort to mimic the oxoiron(IV) intermediates involved in the catalytic cycles of non-heme iron oxygenases.[1] Of the eighty or so complexes characterized, most are found in the $S=1$ ground spin state, unlike the $S=2$ intermediates described for the enzymes. One striking exception is the $S=2$ $[Fe^{IV}(O)(TQA)(L)]^{2+}$ (TQA = tris(2-quinolylmethyl)amine) complex, which exhibits the fastest cyclohexane oxidation rate found thus far for a synthetic Fe^{IV}=O complex.[2] It is proposed that the steric effects of the quinoline donors increase the Fe–N bond lengths, thereby weakening the iron(IV) ligand field to afford the observed $S=2$ ground state.[3] Due to its thermal instability ($t_{1/2}=15$ min in MeCN at −40 °C), it has not been possible to obtain the crystal structure of this highly reactive $S=2$ complex to support this geometric or electronic structure–reactivity correlation.

We have thus embarked on a systematic effort to compare the structure and reactivity of a series of Fe^{IV}(O)(N5) complexes to determine whether such a correlation can be discerned. As a starting point, we have chosen $[Fe^{IV}(O)(N4Py)]^{2+}$ (**1** in Scheme 1), the second oxoiron(IV) complex to be crystallographically characterized, which is relatively stable ($t_{1/2}=60$ h at 25 °C).[4] Variants of the N4Py ligand are known, wherein the two pyridine donors on the bis(pyridyl-2-methyl)amine half are replaced either by *N*-methylbenzimidazole or quinoline (Scheme 1). Complex **2** has been synthesized by Mitra et al.[5] and many of its properties described; however, no structural data is available for this complex. Complex **3** had hitherto not been reported, although the corresponding Mn^{IV}(O) complex and some of its properties have been described by Massie et al.[6] In addition, Sahu et al.[7] have reported the crystal structure of **4**, wherein 2,6-difluorophenyl groups replace the 6-H′s of the pyridines on the bis(pyridyl)methylamine half of the N4Py ligand (Scheme 1). Herein we present the crystal structures of **2** and **3** and compare their spectroscopic and reactivity properties with those of **1**, particularly with respect to their ability to

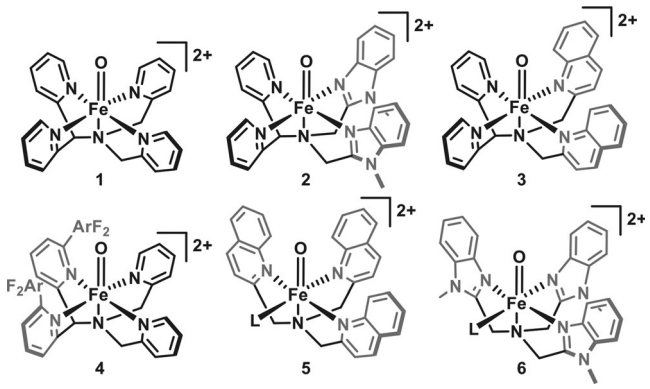

Scheme 1. The oxoiron(IV) complexes evaluated in this work.

[*] W. Rasheed, Dr. A. Draksharapu, S. Banerjee, Dr. V. G. Young Jr., Prof. Dr. L. Que, Jr.
Department of Chemistry and Center for Metals in Biocatalysis
University of Minnesota
Minneapolis, MN 55455 (USA)
E-mail: larryque@umn.edu
R. Fan, Prof. Dr. Y. Guo
Department of Chemistry
Carnegie Mellon University
Pittsburgh, PA 15213 (USA)
E-mail: ysguo@andrew.cmu.edu
Dr. M. Ozerov, Dr. J. Nehrkorn, Dr. J. Krzystek
National High Magnetic Field Laboratory (NHMFL), Florida State University
Tallahassee, FL 32310 (USA)
Prof. Dr. J. Telser
Department of Biological, Chemical and Physical Sciences
Roosevelt University
Chicago, IL 60605 (USA)
E-mail: jtelser@roosevelt.edu
Supporting information and the ORCID identification number(s) for the author(s) of this article can be found under: https://doi.org/10.1002/anie.201804836.

carry out H-atom transfer (HAT) from substrates with C–H bonds. A structural rationale for the much higher reactivity observed for **3** relative to **1** is presented.

Complexes **2** and **3** can be generated by treating CH_3CN/H_2O solutions of the corresponding iron(II) precursors with 4 equivalents of ceric ammonium nitrate (CAN) as the oxidant.[8] Subsequent addition of excess sodium perchlorate to the reaction mixtures results in the precipitation of solids, which can be recrystallized for crystallographic analysis (Figure 1; see Supporting Information for further experimental details). At 25 °C, 1 mM MeCN solutions of these complexes have $t_{1/2} \approx 2.5$ h, which is about 20-fold shorter than for the parent complex **1**. ESI-MS analysis of these solutions reveals major peaks at *m*/*z* 272.58 and 269.50 for **2** and **3**, values expected for the dicationic $[Fe^{IV}(O)(L)]^{2+}$ complexes (Figure S5).

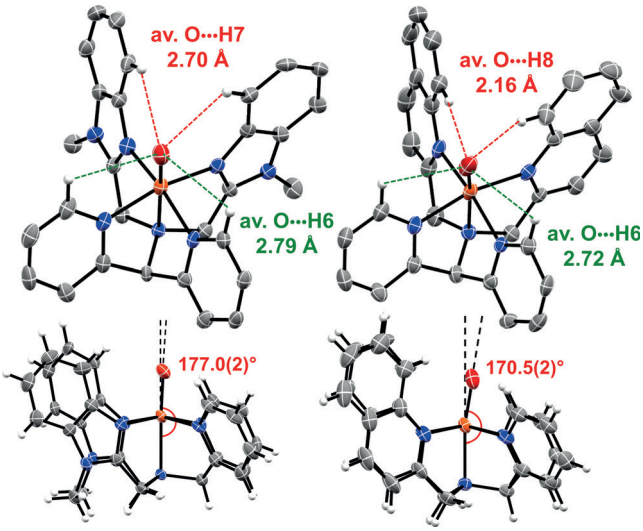

Figure 1. Front and side views of the ORTEP plots of **2** (left) and **3** (right), shown with thermal ellipsoids set at 50% probability. Water molecules, counterions, and select H atoms have been removed for clarity. The dotted line shows the tilt from the Fe–N_{am} axis. See Table 1 and Supporting Information for more crystallographic details and CCDC numbers.

Complexes **1**–**3** exhibit near-IR absorption bands (Figure 2a), assigned previously in the case of **1** ($\lambda_{max} = 695$ nm) to ligand field transitions.[9] For **2** and **3**, the absorbance maxima red-shift to 725 and 770 nm, respectively, suggesting a progressive weakening of the ligand field strength as two pyridine donors are replaced by *N*-methylbenzimidazoles (in **2**) and quinolines (in **3**). For **3**, this notion is further manifested by the appearance of higher-wavelength shoulders at 890 and 930 nm, similar to features observed for $[Fe^{IV}(O)(TMC)(X)]^+$ complexes (TMC = 1,4,8,11-tetramethyl-1,4,8,11-tetraazacyclotetradecane) when the axial MeCN ligand is replaced by anions.[10] Complexes **2** and **3** display ν(Fe=O) features at 842 and 834 cm^{-1}, respectively (Figure 2b, and Figures S6–S8 in the Supporting Information), compared to 843 cm^{-1} for **1**,[8] showing that only the introduction of quinolines in **3** has an effect on ν(Fe=O).

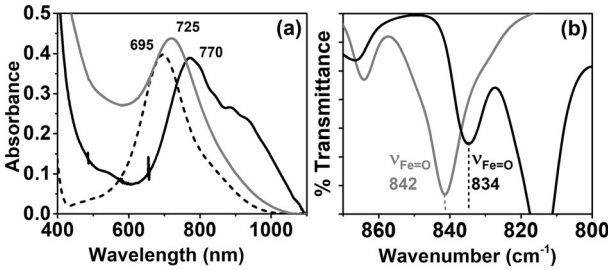

Figure 2. a) Near-IR features of **1** (dashes), **2** (gray), and **3** (black) in 1 mM CH_3CN. b) Fourier transform infrared (FTIR) spectra of **2** (gray) and **3** (black).

Complexes **2** and **3** exhibit Mössbauer spectra with parameters quite similar to those for **1** (Table 1; Figures S9,S10), and those of **2** match those reported by Mitra et al.[5] Their behavior in applied magnetic fields (Figure S10) indicates that they are typical of $S = 1$ non-heme oxoiron(IV) complexes described in the past fifteen years.[1a,11] High-frequency and -field EPR (HFEPR) and frequency-domain spectroscopy with applied fixed magnetic fields (FIR magnetic spectroscopy or FIRMS) have also been found to be useful for characterizing the electronic structures of iron(IV) complexes (Figures S11–S14).[12,13] These techniques are optimally performed on 25–50 mg powder samples,[13a] although frozen solution studies are feasible in certain cases.[13b] Fortunately, **2** and **3** are relatively stable solids that allow the determination of their zero-field splitting (zfs) parameters (axial, *D*; rhombic, *E*) with high precision by concerted use of these two complementary techniques. FIRMS provides a direct measure of the zfs in these complexes by observation

Table 1: Structural and spectroscopic properties of oxoiron(IV) complexes.

Complexes	**1**[a]	**2**[b]	**3**	**4**[c]
r(Fe=O) [Å]	1.639(5)	1.656(4)	1.677(5)	1.6600(16)
r(Fe-$N_{pyridine}$) [Å]	1.964(5)	1.995(5)	2.023(4)	2.0269(17)
		1.983(5)	2.022(4)	2.0408(17)
r(Fe-$N_{heterocycle}$) [Å][b]	1.949(5)	1.950(5)	2.073(4)	1.9730(18)
		1.954(5)	2.067(4)	1.9771(18)
r(Fe-N_{amine}) [Å]	2.033(8)	2.115(6)	2.084(4)	2.0511(17)
av. *r*(Fe-N) [Å]	1.972	1.999	2.053	2.014
∡N_{amine}-Fe-O [°]	179.4(3)	177.0(2)	170.5(2)	177.40(8)
∡$N_{eq.\ plane}$-Fe-O [°]	89.4	88.3	82.4	86.9
ν(Fe=O) [cm^{-1}][d]	843	842	833	n. d.
δ [$mm\,s^{-1}$][a]	−0.04	−0.02	0.03	0.03[7]
ΔE_Q [$mm\,s^{-1}$][a]	0.93	1.36	0.56	0.54
D [cm^{-1}] (MB)	24(2)[14]	25(1)	26(2)	23[7]
D [cm^{-1}] (HFEPR and FIRMS)	22.05(5)[13a]	23.3(1)	24.3(1)	n. d.
λ_{max} [nm]	695	725	770	750[7]
(ε, M^{-1}, cm^{-1})	(400)	(450)	(380)	(250)

[a] Data from Refs. [4, 8a,b, 13a, 14] as noted in each case. [b] Data for **2** from Ref. [5], except for its crystal structure, *D* value and Fe=O stretch reported herein. [c] Data for **4** from Ref. [7]. The modified pyridyl rings in **4** are on the bis(pyridyl-2-methyl)amine half of the ligand (Scheme 1). [d] **2** and **3** from FTIR and **1** from resonance Raman spectroscopy. MB: Mössbauer. n.d.: not determined.

of the $|S, M_S\rangle = |1, 0\rangle \leftrightarrow |1, \pm 1\rangle$ transition (Figures S13,S14), while HFEPR provides complementary information (Figures S11,S12) without the complication of non-magnetic vibrations (phonons) that are also found in this very low frequency region of interest. We have found D to increase from 22.05 cm^{-1} for **1**[13a] to 23.3 and 24.3 cm^{-1} for **2** and **3**, respectively, with $E \approx 0$ in each case. This trend of increasing D suggests a progressive decrease in the energy gap between the ground $S = 1$ and the excited spin states, as these excited states contribute to the zfs in inverse proportion to their relative energies above the ground state.

Key data for **2** and **3** from their crystal structures (Figure 1) are listed in Table 1 and compared to those of the parent complex **1** and the related complex **4**. Complexes **1**–**3** have Fe=O bonds that lengthen from 1.639(5) Å in **1** to 1.656(4) and 1.677(5) Å in **2** and **3**, respectively, as two of the pyridines in **1** are replaced by larger heterocycles, *N*-methylbenzimidazoles in **2** and quinolines in **3**. The average Fe–N bond length concomitantly increases from 1.972 Å in **1** to 1.999 Å in **2** and 2.053 Å in **3**. These trends are also observed for **4**, which differs from **2** and **3** in that a different pair of pyridines is modified (Scheme 1). For the substitution in **4**, the phenyl rings are found to rotate about the C–C bonds connecting the phenyl ring to the pyridine such that they become approximately perpendicular to the bound pyridines, thereby minimizing unfavorable steric interactions. When the bond metrics for **4** are considered relative to those for **1**–**3**, **4** falls between **2** and **3** (Table 1).

The trends among complexes **1**–**4** discussed above very likely arise from the steric and electronic effects of the heterocycles that replace two of the pyridine donors on the N4Py framework. The steric effect is best demonstrated in the crystal structure of **3**, which shows that the H8 atoms of the two quinolines are on average only about 2.16 Å away from the oxo atom (Figure 1 and Table S4). For comparison, the corresponding H7 atoms of the benzimidazole donors are much farther away, at 2.70 Å from the oxo atom in **2**, a distance similar to those found for the H6 protons of the unsubstituted pyridine rings in **1**–**4** (which range from ca. 2.5–2.8 Å). As a consequence, the quinoline H8 protons would appear to exert a steric effect that results in a tilt of the Fe=O unit in **3** away from the quinoline rings, leading to the observed N_{am}-Fe-O angle of 170.5° (see Figure 1). (This observed tilt was anticipated by DFT calculations on the corresponding Mn^{IV}(O) complex in Ref. [6].) For comparison, the N_{am}-Fe-O angles observed for **1**, **2**, and **4** are much closer to that for a linear arrangement, namely 179.4(3)°, 177.0(2)° and 177.40(8)°, respectively. Consistent with this proposed steric effect, the slight tilts found for **2** and **4** relative to **1** are oriented away from the bulkier heterocycles.

The basicity of the heterocycles increases from quinoline to pyridine to benzimidazole, and this effect on the bond lengths of the equatorial ligands can be seen in the short benzimidazole Fe–N bond lengths of 1.950(5) Å in **2**.[15] The stronger binding of benzimidazole induces a *trans* effect that increases the equatorial pyridine Fe–N bond lengths. This, along with the longer axial Fe–N bond length of 2.115(5) Å, increases the average Fe–N bond length for complex **2**. Steric effects in complex **3** are responsible for its longer Fe–N bond lengths and outweigh the electronic effects of quinolines.

The structural differences in the **1**–**3** series are also reflected in their HAT and OAT rates. Figure 3a shows plots

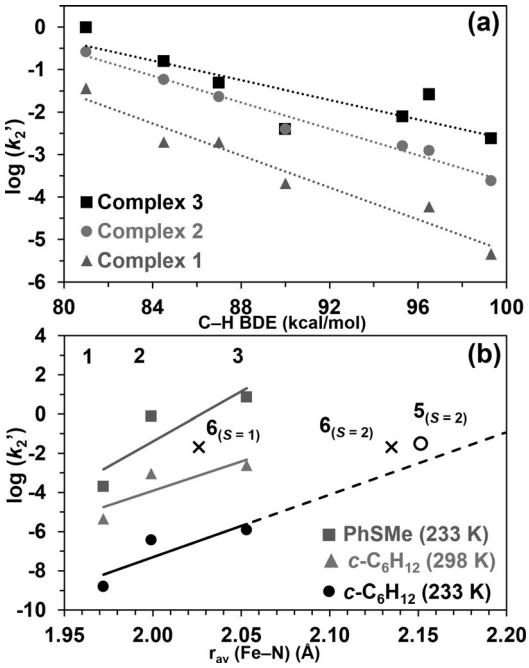

Figure 3. a) Evans–Polanyi plot for **3** at 25 °C, and previously published data for **1**[4a] and **2**.[5] b) Correlation of $\log k_2'$ values for thioanisole at −40 °C (squares) and cyclohexane at 25 °C (triangles) and at −40 °C (circles) versus the average Fe–N bond lengths for **1**–**3** based on crystallographic data. The bottom plot is extended to $r_{av} = 2.20$ Å to determine whether this correlation also holds true for the $S = 2$ complex **5** (open circle) and complex **6** (crosses). The average Fe–N bond lengths for **5** and **6** were obtained from DFT-optimized 6-coordinate structures in $S = 1$ or 2 spin states.

of $\log k_2'$ values (where k_2' is k_2 divided by the number of equivalent substrate C–H bonds that can be attacked) versus the C–H bond dissociation energy for **1**–**3**, which reveal reasonably linear correlations for the three sets of data, as observed previously for a number of oxoiron(IV) complexes.[1d] The rate differences among the three complexes become larger for substrates with stronger C–H bonds, resulting in a decrease in the slopes from **1** to **2** and then to **3**. The oxygen-atom transfer rates to thioanisole at −40 °C also increase from **1** to **3**, by over four orders of magnitude after extrapolating the value for **1** to −40 °C from its Eyring parameters (Figure S22).

Figure 3b shows a remarkable correlation between $\log k_2'$ values and the average length of all five Fe–N bonds found in complexes **1**–**3**. Such a correlation has not previously been possible due to the paucity of crystal structures of related non-heme oxoiron(IV) complexes. With the structures of **2** and **3** reported herein, in combination with the previously reported structure of **1**,[4b] we now have three complexes with the *same* polydentate ligand framework with which to relate structure and function. Indeed we find that the substrate oxidation rates of **1**–**3** increase as the average Fe–N bond lengthens for the

oxoiron(IV) oxidant (Figure 3b, Table S8), so the oxoiron(IV) complex with the longer average Fe–N bond length gives rise to the more reactive complex.

As a simple interpretation, the observed correlation could reflect an increase in the electrophilicity of the $S=1$ Fe^{IV}=O unit with the increase in the average Fe–N bond length. A more complex argument to rationalize the HAT trends would involve the two-state reactivity (TSR) model proposed by Shaik,[16] where the lengthening of the average Fe–N bond would weaken the ligand field and thus decrease the energy gap between the $S=1$ ground state and the $S=2$ excited state that governs the reactivity of the Fe^{IV}=O unit. This notion is supported by our HFEPR measurements, which show an increase in the zfs parameter D in 1-cm^{-1} increments from **1** to **3** (Table 1). The increase in the zfs is purely an increase in D as the rigorously axial nature ($E \approx 0$) of the electronic structure of the oxoiron(IV) unit is maintained upon going from **1** to **3**, despite the tilting of the Fe=O unit. Thus the reactivity trend observed for **1**–**3** can also be understood using the TSR model.

To put this structure/reactivity correlation into a broader context, we have checked where the cyclohexane hydroxylation rates for the $S=2$ $[Fe^{IV}(O)(TQA)(NCMe)]^{2+}$ (**5**) and $S=1$ $[Fe^{IV}(O)(Me_3NTB)(NCMe)]^{2+}$ (**6**; Scheme 1) complexes might fall on this plot. These two complexes, respectively have three quinoline and benzimidazole donors and are the most reactive oxoiron(IV) complexes found to date.[2,17] As HAT rates for **5**[2] and **6**[17] have been reported only at −40 °C, k_2 values for **1**–**3** at −40 °C were obtained by extrapolation from Eyring plots for cyclohexane oxidation for proper comparison (Figures S18–S22, Tables S10,S11). Complexes **5** and **6** have not been crystallized, so the average Fe-N distances needed for the correlation plot in Figure 3b had to be obtained from DFT calculations (Table S9).[2,17] To our surprise, the point for **5** actually falls close to the line defined by the HAT values for **1**–**3**, despite the fact that **5** is a bona fide $S=2$ complex[2] and is thus unlike the $S=1$ complexes **1**–**3** used to define the correlation line. This apparent correlation raises the prospect that the average Fe–N bond length in oxoiron(IV) complexes may reflect the electrophilicity of the Fe^{IV}=O unit.

Complex **6** represents an intriguing test case, as it has been characterized by Nam and co-workers using Mössbauer spectroscopy to have an $S=1$ ground spin state at 80 K (−193 °C) and below, but exhibits HAT rates at −40 °C comparable to those of $S=2$ complex **5**.[2,17] When its cyclohexane k_2 value (represented by a cross) is added to the plot of HAT rates at −40 °C in Figure 3b using the average Fe–N distance of 2.135 Å calculated for the MeCN-bound $S=2$ complex, the point falls close to the line. In contrast, a poor correlation is found when the shorter average Fe–N distance of 2.026 Å calculated for the corresponding $S=1$ complex is used. This comparison supports speculation by Nam and co-workers that **6** becomes $S=2$ at −40 °C to account for its observed higher HAT reactivity.[17] Nam's model however requires **6** to be a trigonal bipyramidal complex at this temperature to become high spin. With this geometry, the calculated average Fe-N distance shortens to 2.042 Å, and the plotted point would be too short to fall close to the line. A significant shortening of the average Fe-N distance is also predicted for trigonal bipyramidal **5**, and the plotted point would be similarly incongruent with the correlation.[2] Further studies are thus required to rationalize the unexpectedly high reactivity of **6**.

In summary, **2** and **3** represent the first oxoiron(IV) complexes with *N*-methylbenzimidazole or quinoline donors to be crystallographically characterized, shedding light on how these modifications can affect the Fe=O environment. Based on this work, it is evident that the quinolyl donors of **3** exert steric effects that increase the average Fe–N bond length and tilt the Fe=O unit away from these donors, resulting in higher HAT and OAT rates relative to **1** and **2**. Increasing the number of quinolines to three in **5** further lengthens the average Fe–N distance and makes the Fe=O unit high spin, enhancing its reactivity and lending credence to the correlation between reactivity and average Fe–N distance shown in Figure 3b.

Acknowledgements

This work was supported by grants from the U.S. National Science Foundation (CHE-1665391 to L.Q. and CHE-1654060 to Y.G.). The National High Magnetic Field Laboratory is supported by U.S. National Science Foundation through Cooperative Agreement DMR-1644779 and the State of Florida. The Bruker-AXS D8 Venture Diffractometer was purchased through a grant from NSF/MRI 1229400 and the University of Minnesota. We thank Prof. Steven Kass for the use of their FTIR spectrometer and the reviewers for their helpful suggestions.

Conflict of interest

The authors declare no conflict of interest.

Keywords: hydrogen atom transfer (HAT) · non-heme iron complexes · oxoiron(IV) complexes · two-state reactivity

How to cite: *Angew. Chem. Int. Ed.* **2018**, *57*, 9387–9391
Angew. Chem. **2018**, *130*, 9531–9535

[1] a) A. R. McDonald, L. Que, Jr., *Coord. Chem. Rev.* **2013**, *257*, 414–428; b) W. Nam, Y.-M. Lee, S. Fukuzumi, *Acc. Chem. Res.* **2014**, *47*, 1146–1154; c) X. Engelmann, I. Monte-Pérez, K. Ray, *Angew. Chem. Int. Ed.* **2016**, *55*, 7632–7649; *Angew. Chem.* **2016**, *128*, 7760–7778; d) J. E. M. N. Klein, L. Que in *Encyclopedia of Inorganic and Bioinorganic Chemistry*, Wiley, Hoboken, **2016**, https://doi.org/10.1002/9781119951438.eibc9781119952344.

[2] A. N. Biswas, M. Puri, K. K. Meier, W. N. Oloo, G. T. Rohde, E. L. Bominaar, E. Münck, L. Que, *J. Am. Chem. Soc.* **2015**, *137*, 2428–2431.

[3] M. Puri, L. Que, *Acc. Chem. Res.* **2015**, *48*, 2443–2452.

[4] a) J. Kaizer, E. J. Klinker, N. Y. Oh, J.-U. Rohde, W. J. Song, A. Stubna, J. Kim, E. Münck, W. Nam, L. Que, Jr., *J. Am. Chem. Soc.* **2004**, *126*, 472–473; b) E. J. Klinker, J. Kaizer, W. W. Brennessel, N. L. Woodrum, C. J. Cramer, L. Que, Jr., *Angew.*

Chem. Int. Ed. **2005**, *44*, 3690 – 3694; *Angew. Chem.* **2005**, *117*, 3756 – 3760.
[5] M. Mitra, H. Nimir, S. Demeshko, S. S. Bhat, S. O. Malinkin, M. Haukka, J. Lloret-Fillol, G. C. Lisensky, F. Meyer, A. A. Shteinman, W. R. Browne, D. A. Hrovat, M. G. Richmond, M. Costas, E. Nordlander, *Inorg. Chem.* **2015**, *54*, 7152 – 7164.
[6] A. A. Massie, M. C. Denler, L. T. Cardoso, A. N. Walker, M. K. Hossain, V. W. Day, E. Nordlander, T. A. Jackson, *Angew. Chem. Int. Ed.* **2017**, *56*, 4178 – 4182; *Angew. Chem.* **2017**, *129*, 4242 – 4246.
[7] a) S. Sahu, M. G. Quesne, C. G. Davies, M. Dürr, I. Ivanović-Burmazović, M. A. Siegler, G. N. L. Jameson, S. P. de Visser, D. P. Goldberg, *J. Am. Chem. Soc.* **2014**, *136*, 13542 – 13545; b) S. Sahu, B. Zhang, C. J. Pollock, M. Dürr, C. G. Davies, A. M. Confer, I. Ivanović-Burmazović, M. A. Siegler, G. N. L. Jameson, C. Krebs, D. P. Goldberg, *J. Am. Chem. Soc.* **2016**, *138*, 12791 – 12802.
[8] a) Y.-M. Lee, S. N. Dhuri, S. C. Sawant, J. Cho, M. Kubo, T. Ogura, S. Fukuzumi, W. Nam, *Angew. Chem. Int. Ed.* **2009**, *48*, 1803 – 1806; *Angew. Chem.* **2009**, *121*, 1835 – 1838; b) A. Draksharapu, D. Angelone, M. G. Quesne, S. K. Padamati, L. Gómez, R. Hage, M. Costas, W. R. Browne, S. P. de Visser, *Angew. Chem. Int. Ed.* **2015**, *54*, 4357 – 4361; *Angew. Chem.* **2015**, *127*, 4431 – 4435; c) A. Draksharapu, W. Rasheed, J. E. M. N. Klein, L. Que, *Angew. Chem. Int. Ed.* **2017**, *56*, 9091 – 9095; *Angew. Chem.* **2017**, *129*, 9219 – 9223.
[9] A. Decker, J.-U. Rohde, L. Que, Jr., E. I. Solomon, *J. Am. Chem. Soc.* **2004**, *126*, 5378 – 5379.
[10] T. A. Jackson, J.-U. Rohde, M. S. Seo, C. V. Sastri, R. DeHont, A. Stubna, T. Ohta, T. Kitagawa, E. Münck, W. Nam, L. Que, Jr., *J. Am. Chem. Soc.* **2008**, *130*, 12394 – 12407.
[11] A. Chanda, X. Shan, M. Chakrabarti, W. C. Ellis, D. L. Popescu, F. Tiago de Oliveira, D. Wang, L. Que, Jr., T. J. Collins, E. Münck, E. L. Bominaar, *Inorg. Chem.* **2008**, *47*, 3669 – 3678.
[12] J. Telser, J. Krzystek, A. Ozarowski, *J. Biol. Inorg. Chem.* **2014**, *19*, 297 – 318.
[13] a) J. Krzystek, J. England, K. Ray, A. Ozarowski, D. Smirnov, L. Que, Jr., J. Telser, *Inorg. Chem.* **2008**, *47*, 3483 – 3485; b) L. Bucinsky, G. T. Rohde, L. Que, A. Ozarowski, J. Krzystek, M. Breza, J. Telser, *Inorg. Chem.* **2016**, *55*, 3933 – 3945; c) L. Bucinsky, M. Breza, W.-T. Lee, A. K. Hickey, D. A. Dickie, I. Nieto, J. A. DeGayner, T. D. Harris, K. Meyer, J. Krzystek, A. Ozarowski, J. Nehrkorn, A. Schnegg, K. Holldack, R. H. Herber, J. Telser, J. M. Smith, *Inorg. Chem.* **2017**, *56*, 4751 – 4768.
[14] M. P. Jensen, M. Costas, R. Y. N. Ho, J. Kaizer, A. Mairata i Payeras, E. Münck, L. Que, Jr., J.-U. Rohde, A. Stubna, *J. Am. Chem. Soc.* **2005**, *127*, 10512 – 10525.
[15] M. Lõkov, S. Tshepelevitsh, A. Heering, P. G. Plieger, R. Vianello, I. Leito, *Eur. J. Org. Chem.* **2017**, 4475 – 4489.
[16] a) E. J. Klinker, S. Shaik, H. Hirao, L. Que, Jr., *Angew. Chem. Int. Ed.* **2009**, *48*, 1291 – 1295; *Angew. Chem.* **2009**, *121*, 1317 – 1321; b) D. Mandal, D. Mallick, S. Shaik, *Acc. Chem. Res.* **2018**, *51*, 107 – 117.
[17] a) M. S. Seo, N. H. Kim, K.-B. Cho, J. E. So, S. K. Park, M. Clémancey, R. Garcia-Serres, J.-M. Latour, S. Shaik, W. Nam, *Chem. Sci.* **2011**, *2*, 1039 – 1045; b) H. Bae Seong, S. Seo Mi, Y. M. Lee, K. B. Cho, W. S. Kim, W. Nam, *Angew. Chem. Int. Ed.* **2016**, *55*, 8027 – 8031; *Angew. Chem.* **2016**, *128*, 8159 – 8163; c) N. Y. Lee, D. Mandal, S. H. Bae, M. S. Seo, Y.-M. Lee, S. Shaik, K.-B. Cho, W. Nam, *Chem. Sci.* **2017**, *8*, 5460 – 5467.

Manuscript received: April 25, 2018
Accepted manuscript online: June 7, 2018
Version of record online: June 28, 2018

